Please note that this article was first published on 29th June 2021 without any associated ESI.
This ESI was added on 4th October 2021.

Supplementary Information

Enhanced Photoluminescence of Silicon Quantum Dots in the Presence of both Energy Transfer Enhancement and Emission Enhancement Mechanisms Assisted by Double Plasmon Modes of Gold Nanorods

Jiahao Cao, Hanjie Zhang, Xiaodong Pi, Dongsheng Li and Deren Yang**

State Key Laboratory of Silicon Materials and School of Materials Science and Engineering, Zhejiang University, Hangzhou 310027, P.R. China

Core-shell structures have been widely studied for photocatalysis, plasmon-enhanced spectroscopy, [1] biotechnology, and solar cells. The developments in the field of (plasmonic metal)/semiconductor hybrid nanostructures are comprehensively described in Ruibin Jiang's review.[2] Our initial research was to regulate the energy transfer between quantum dots through core-shell structure. Similar core-shell structures using CdSe QDs with different size as donors and acceptors have also been prepared for comparison utilizing the method in Khanal's work.[3] A patent[4] and the work using silver nanoparticles (Ag NPs) with single broad resonance peak to regulate the energy transfer between Si QDs were published in 2019[5], where Minoru Fujii's works on energy transfer between Si QDs were discussed and cited.[6-8] To demonstrate the advantages of double resonance peaks of Au NRs, GNR@SiO_2-QDs structures were prepared. We note the recently published article by Pavelka et al. "Optimizing plasmon enhanced luminescence in silicon nanocrystals by gold nanorods" Nanoscale, 2021, 13, 5045), which proposed an optimized fabrication of gold nanorod-silicon nanocrystal

core–shell nanoparticles by electrostatic adsorption. This is similar to Minoru Fujii's previous work in 2015 (references 27, 28 in Pavelka's work),[9, 10] with the silica shell as a tunable spacer and investigated the spacer thickness dependence of photoluminescence intensity enhancement using a combination of experimental measurements and numerical simulations.

S1. Preparation of Si QDs

50 mL mixture of Si QDs (1 mg/mL) and methanol was placed in a polytetrafluoroethylene (PTFE) beaker. 5 mL aqueous hydrofluoric acid (HF, 40%) was added with stirring to remove the surface oxide of Si QDs. (Caution: Hydrofluoric acid can be extremely dangerous and must be handled with great care.) The resulting H–Si QDs were obtained by centrifugation at 10000 rpm for 3 min. It should be noted that Si−H bonds at the QD surface are vulnerable to oxidation as they are exposed in air. The mixture was further washed with anhydrous toluene and centrifuged twice and dispersed in 15 mL anhydrous toluene. For more details of the synthesis employing nonthermal plasma system, hydrogen passivation and surface modification of silicon quantum dots, you can you can refer to the work of L. Mangolini[11] and our cooperator professor Xiaodong Pi. [12–14]

Hydride terminated Si-NCs were transferred to a Schlenk flask containing 15 mL dry toluene. 0.15 g of PCl_5 was added to the hydride Si-NCs with stirring for 1 hour at 40℃ under Ar atmosphere. Toluene and byproducts were removed in vacuo. 15 mL dry toluene and 0.1 g of octadecylamine were added to the reaction flask. The reaction mixture was heated at 40℃ for 12 hours. The flask was cooled to room temperature and the solution was transferred to a separatory funnel and washed with distilled water thrice. The toluene layer was filtered through a hydrophobic PTFE filter, and the Si QDs are then dissolved in 5 mL chloroform.

Finally, the addition of amine functionalized Si QD was performed dropwise to activated silica-coated metal solution with vigorous stirring for 12 hours. The concentration of Si QDs in chloroform is about 10^{-5} mol/L. THF(>99%) and

chloroform(99.8%) are purchased from Sinopharm Chemical Reagent Co., Ltd. Since Si QDs are particularly susceptible to oxidation, chloroform is a better choice. The hybrid superstructures are purified from excess, unbound quantum dots by centrifugation and redispersion in 5 mL chloroform. Use of an excess of QDs results in reproducible and uniform loading on the SiO_2 surface; lower loading levels (i.e., number of QDs per GNR) can be achieved without loss of uniformity by reducing the relative amount of APTES used during functionalization. Note that "an excess of QDs" means that the area occupied by Si QDs is larger than the surface area of GNR@SiO_2. (similar with Pavelka's work, the total footprint of Si QDs is larger than the total surface of GNR@SiO_2). In a typical attachment process, 10^{-11} moles of GNR@SiO_2 were mixed with 10^{-8} moles of Si QDs in 5 mL chloroform.

S2. The size of donor and acceptor Si QDs

The size of Si QDs in the plasma synthesis reactor can be tailored both by the SiH_4 partial pressure and the residence time of the gas in the plasma zone. In addition, size selection is further carried out to obtain Si QDs of different size by means of density-gradient ultracentrifugation. [15, 16] Silicon quantum dots of different sizes are chosen as donors (3.1 ± 0.5 nm) and acceptors (4.9 ± 0.7 nm). The high-resolution TEM images and size distributions are shown in figure S1.

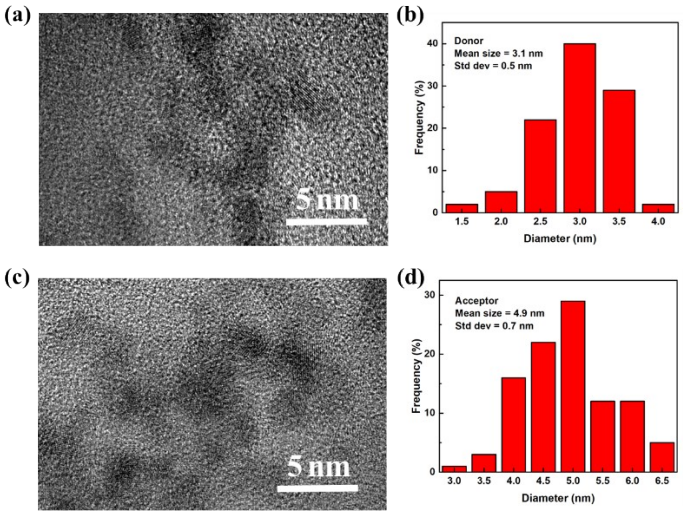

Figure S1. High-resolution TEM images and size distributions of donor(a, b) and acceptor(c, d) Si QDs

S3. The photoluminescence of Si QDs

The PL spectra of donor and acceptor are shown in figure 1b in the paper. The emission peaks of donors and acceptors are 612 nm and 690 nm respectively, which are not affected by the excitation wavelength, and the lifetimes show microsecond excited state lifetimes. It is well known that the quantum confinement effect of Si QDs renders the relationship between *Eg* and *d* (QD size) to comply with an effective mass approximation (EMA).[17-19] The PL lifetimes and the redshift of emission peak with the increase size of Si QDs are consistent with the generally observed PL dynamics of quantum-confined Si QDs. Thus, we believe that the red photoluminescence originates from the band gap transition of quantum-confined Si QDs.

As we all know, the luminescence of quantum dots is affected by factors such as size, defects, surface passivation functional groups and surface coverage rate. In Dasog's work, [20] the dodecylamine Si-NCs photoluminesce in the blue spectral region, which showed excitation wavelength dependence, and the excited-state lifetimes showed fast decay with several nanosecond measured at 470 nm. Dasog proposed that nitrogen atoms on the surface of Si NCs and oxygen in the air work together and the blue PL results from a charge transfer state involving silicon oxynitride type species. At this time, the carriers in the Si NCs prefer to be transferred to the luminescent center on the surface to recombine, rather than recombine through the band gap transition, and this process requires a shorter time, which shows nanosecond lifetime.

There are several factors that cause the difference in luminous performance. First of all, the synthesis methods of Si QDs are different. In Dasog's work, oxide-embedded Si-NCs are readily obtained via disproportionation of commercially available HSQ at high temperature (ca. 1100 ℃), which may contribute to the formation of oxidation-induced defects on the surface of Si NCs. Si NCs synthesized by this method have relatively poor crystallinity and size uniformity, showing a broader emission peak, while silicon nanocrystals with air-stable full-visible-spectrum emission are

synthesized in nonthermal SiH_4-based plasma system.[21] Structural and optical characterization indicates that the emission in the red-to-green range is based on the recombination of quantum-confined excitons in Si-NCs, while the blue emission originates from oxidation-induced defect states. This is somewhat similar to our work and Dasog's work. Secondly, the chemical reagents used for surface modification of quantum dots are different. In our work, octadecylamine is used to passivate the surface of silicon quantum dots. It has longer carbon chains, the entanglement of which is more conducive to inhibiting oxidation from the oxygen in air. At the same time, because the steric hindrance prevents the Si QDs surface from being completely covered, the longer carbon chains of octadecylamine also reduce the surface coverage rate of silicon quantum dots, allowing part of chlorine to be retained. Pro. Xidong Pi proposed that C and F play a role in preventing the formation of oxygen-related intra-bandgap energy levels.[21] Since chlorine and fluorine have similar chemical properties, we believe that the chlorine retained on the surface of Si QDs can also play a role in preventing the generation of oxygen-related charge transfer state involving silicon oxynitride type species. Figure S2 and S3 are FTIR spectra of octadecylamine functionalized Si NCs and dodecylamine functionalized Si NCs. The presence of chlorine on the Si NCs surface is evidenced by the occurrence of the Si-Cl related signal at 550-610 cm^{-1} in figure S2. In addition, larger amount of suboxide at the surface of dodecylamine-Si QDs is confirmed by the observation that the FTIR signal related to Si-O-Si at 950-1150 cm^{-1} is much stronger for dodecylamine-Si NCs than that for octadecylamine-Si NCs, which proves to a certain extent that the chlorine on the surface of Si NCs can inhibit the formation of oxygen-related silicon oxynitride type species. In this case, the red photoluminescence originating from the quantum confinement effect dominates the light-emitting process, which also explains why the silicon quantum dots exhibit a microsecond lifetime.

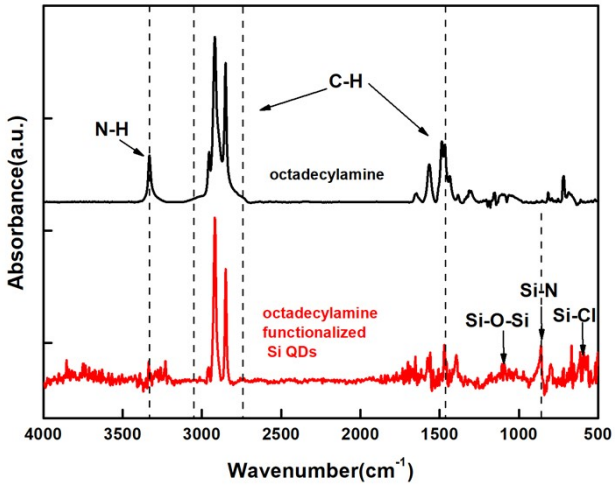

Figure S2. FTIR spectra of octadecylamine and octadecylamine functionalized Si NCs.

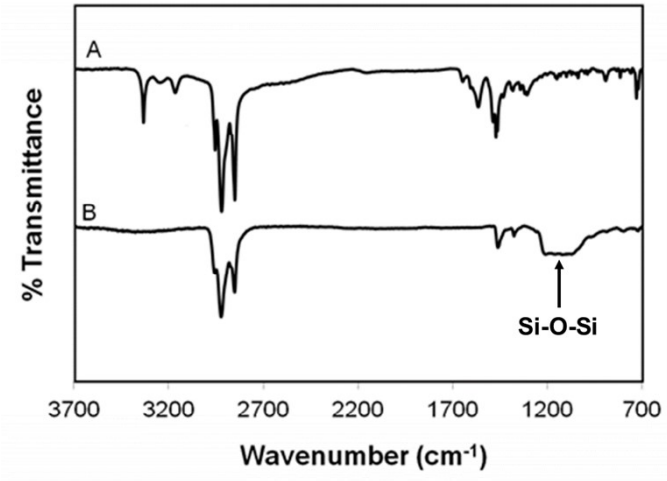

Figure S3. FTIR spectra of (A) dodecylamine and (B) dodecylamine functionalized Si NCs.

S4. The characterization of the core-shell structures

Figure S4 shows the energy dispersive X-ray (EDX) elemental maps of Au and Si in the hybrid nanostructures. Because SiO_2 also contains Si element, it can be seen in figure S4(b) that the central part of the structure has a higher silicon element content, which comes from SiO_2 and the silicon quantum dots attached to the surface, while the Si element at the edge comes from the silicon quantum dots attached to the surface and a very small part of the unbound silicon quantum dots remaining in the solvent.

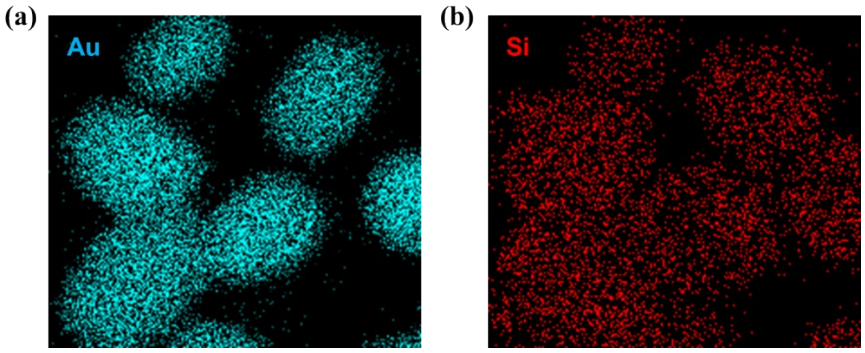

Figure S5. Energy dispersive X-ray (EDX) elemental maps of Au (a) and Si (b) in GNR-SiO_2-Si QDs.

Reference

[1] Saji Thomas Kochuveedu, Taehwang Son, Youmin Lee, Minyung Lee, Donghyun Kim, Dong Ha Kim., Scientific Reports, 2014, 4, 4735.

[2] Ruibin Jiang, Benxia Li, Caihong Fang, and Jianfang Wang., Advanced Materials, 2014, 26, 5274–5309.

[3] Khanal, B. P.; Pandey, A.; Li, L.; Lin, Q. L.; Bae, W. K.; Luo, H. M.; Klimov, V. I.; Pietryga, J. M., ACS Nano 2012, 6, 3832−3840.

[4] Dongsheng Li, Hanjie Zhang, Deren Yang. LSPR (local surface plasmon resonance)-assisted transferring structure capable of giving consideration to different quantum dot energies, and preparation method thereof, China 201810167817.6, 2018-02-28.

[5] J. H. Cao, H. J. Zhang, X. K. Liu, N. Zhou, X. D. Pi, D. S. Li and D. R. Yang, J. Phys. Chem. C, 2019, 123, 23604–23609.

[6] Furuta, K.; Fujii, M.; Sugimoto, H.; Imakita, K., J. Phys. Chem. Lett. 2015, 6, 2761-2766.

[7] Limpens, R.; Lesage, A.; Stallinga, P.; Poddubny, A. N.; Fujii, M.; Gregorkiewicz, T., J. Phys. Chem. C 2015, 119, 19565−19570.

[8] Sugimoto, H.; Furuta, K.; Fujii, M., J. Phys. Chem. C 2016, 120, 24469−24475.

[9] H. Sugimoto, T. Chen, R. Wang, M. Fujii, B. M. Reinhard and L. Dal Negro, ACS Photonics, 2015, 2, 1298–1305.

[10] A. Inoue, M. Fujii, H. Sugimoto and K. Imakita, J. Phys. Chem. C, 2015, 119, 25108–25113.

[11] L. Mangolini, E. Thimsen, U. Kortshagen, *Nano Lett.* **2005**, *5*, 655.

[12] X. D. Pi, Q. Li, D. Li, D. Yang, *Sol. Energy Mater. Sol. Cells* **2011**, *95*, 2941.

[13] Xiangkai Liu, Yuheng Zhang, Ting Yu, Xvsheng Qiao, Ryan Gresback, Xiaodong Pi, Deren Yang, *Part. Part. Syst. Charact.* **2016**, *33*, 44–52.

[14] Xiangkai Liu, Shuangyi Zhao, Wei Gu, Yuting Zhang, Xvsheng Qiao, Zhenyi Ni, Xiaodong Pi, Deren Yang, ACS Appl. Mater. Interfaces 2018, 10, 5959−5966.

[15] M. L. Mastronardi, F. Hennrich, E. J. Henderson, F. Maier-Flaig, C. Blum, J. Reichenbach, U. Lemmer, C. Kübel, D. Wang, M. M. Kappes, G. A. Ozin, *J. Am. Chem. Soc.* **2011**, *133*, 11928.

[16] J. B. Miller, J. M. Harris, E. K. Hobbie, *Langmuir* **2014**, *30*, 7936.

[17]. Efros, A. L., *Soviet Phys. Semiconductors USSR* **1982,** *16*, 772-775.

[18]. Barbagiovanni, E. G.; Lockwood, D. J.; Simpson, P. J.; Goncharova, L. V., *Appl. Phys. Rev.* **2014,** *1*, 011302.

[19]. Trwoga, P. F.; Kenyon, A. J.; Pitt, C. W., *J. Appl. Phys.* **1998,** *83*, 3789-3794.

[20] Mita Dasog, Glenda B. De los Reyes, Lyubov V. Titova, Frank A. Hegmann, Jonathan G. C. Veinot. ACS Nano, 2014, 8, 9, 9636–9648.

[21] X. D. Pi, R. W. Liptak, J. D. Nowak, N. P. Wells, C. B. Carter, S. A. Campbell, U. Kortshagen, Nanotechnology **2018,** 19, 245603.